IOP Publishing
Measurement Science and Technology
Meas. Sci. Technol. 31 (2020) 047003 (6pp)
https://doi.org/10.1088/1361-6501/ab5292

Technical Note

Development of a photo-thermal scan head for high-speed atomic force microscope

Bernard Ouma Alunda[1], Luke Oduor Otieno[1], Sang Joon Park[1], Si Geun Choi[2], Jong Hyoung Kim[2] and Yong Joong Lee[1]

[1] School of Mechanical Engineering, Kyungpook National University, 80 Daehak-ro, Buk-gu, Daegu 41566, Republic of Korea
[2] Extreme Fabrication Technology Group at Korea Institute of Industrial Technology (KITECH), 320 Technosunhwan-ro, Yuga-eup, Dalseong-gun, Daegu 42994, Republic of Korea

E-mail: yjlee76@knu.ac.kr

Received 11 June 2019, revised 28 October 2019
Accepted for publication 30 October 2019
Published 23 January 2020

Abstract

Atomic force microscopy (AFM) is one of the frequently used microscopy techniques to capture high-resolution images in science and engineering. Since the spatial resolution limit of AFM has been mostly reached and no further improvement is likely, much of the recent attention in the development of new AFM has been on improvement of speed. We present a photo-thermal, high-speed atomic force microscope scan head capable of exciting cantilevers photo-thermally and detecting cantilever motions with an optical beam bounce technique. The design features a unique Z-collar that permits direct mounting of a Z-scanner onto a microscope objective lens to achieve a high mechanical bandwidth. We demonstrate the performance of the developed scan head by imaging data tracks of a Blu-ray disk in tapping and contact modes.

Keywords: high-speed atomic force microscopy, optical beam deflection, finite element analysis

(Some figures may appear in colour only in the online journal)

1. Introduction

High-speed atomic force microscopy (AFM) has proven to be a powerful tool for visualizing different phenomena in various research fields such as material science [1, 2], life science [3, 4], chemistry [5, 6] and industry [7, 8]. The instrument has also enabled different surface characterizations and analyses with an exceptional level of spatial resolution in diverse environments. For example, in life science AFM has enabled the visualization of a walking myosin V [9], kinesin molecules [10], bacterial behaviors [11, 12], and determining the morphology of cancer cells [13, 14]. Some of these studies have shown insights into different biological processes that were not previously clarified. Just as a chain is only as strong as its weakest link, AFM's speed is limited by the slowest component in its entire control loop. Achieving high-speed imaging requires innovations in cantilevers, scanners, deflection measurement techniques, and electronic controllers. In the recent past, the development of cantilevers with resonant frequencies higher than 300 kHz helped push the scan speed higher [15–17]. Higher resonant frequency cantilevers were made possible by significantly reducing the size of the cantilevers, thereby reducing the effective mass while increasing the stiffness. Small cantilevers not only allow fast scanning [18, 19] but also limit the force noise, thereby allowing even smaller forces to be detected [20].

However, a way to effectively excite small cantilevers in the MHz regime, especially in a liquid environment, remains a challenge. The presently used cantilever excitation techniques include piezo-acoustic, magnetic [21, 22], Brownian motion

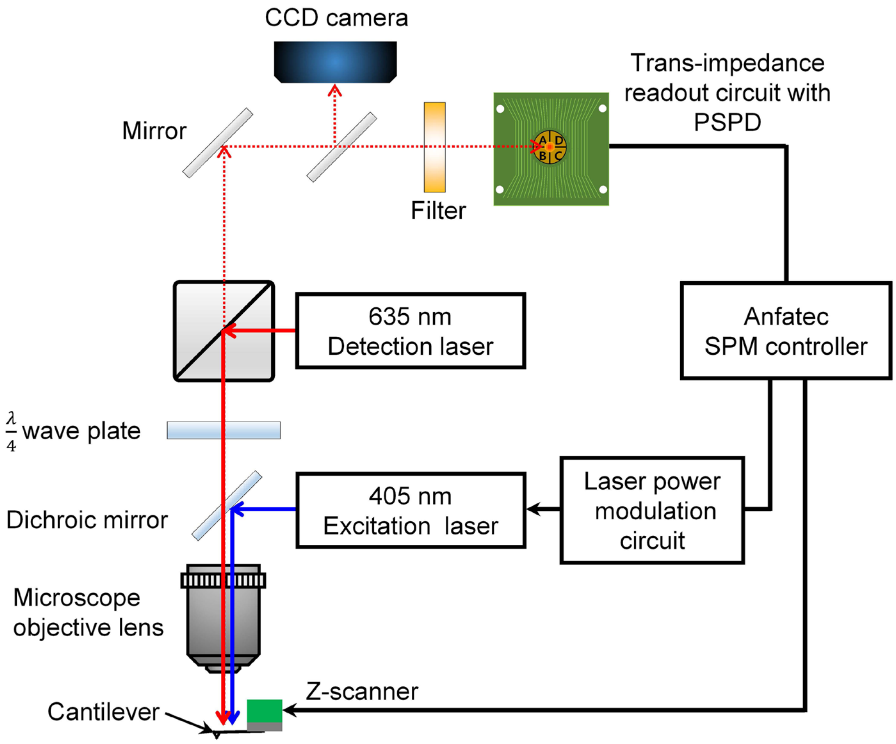

Figure 1. A schematic of the photo-thermal, high-speed atomic microscope (PHS-AFM) scan head with the associated components. PSPD: position-sensitive photodiode, SPM: scanning probe microsocpe.

[23, 24], photo-thermal and electrostatic excitation [25]. The prevalent method adopted by many AFM designs is the piezo-acoustic excitation partly because of its cost effectiveness, ease of implementation, and operation. However, the indirect excitation of the cantilever causes a number of cantilever resonances to appear in liquid environments [26]. Photo-thermal cantilever excitation offers an alternative means of directly driving the cantilever, thus preventing spurious resonances in addition to its wide applicable frequency range [27].

2. Experiments and discussion

2.1. Optics design

A schematic of our home-made photo-thermal, high-speed atomic force microscope scan head (PHS-AFM) is shown in figure 1. In order to implement the photo-thermal excitation of a cantilever in the proposed AFM design, a 30 mW pigtailed laser diode (LP405-SF30, Thorlabs) with a center wavelength of 405 nm was used. The collimation of the laser was achieved by using an adjustable focal point collimator (FC/PC CFC-11X-A, Thorlabs) that allowed a variable output beam diameter. For detection, a 2.5 mW pigtailed laser diode with a center wavelength of 635 nm provided more than enough laser power for the optical beam bounce detection (OBD) technique for cantilever deflection measurements. The detection laser was directed to a collimator (FC230FC-B, Thorlabs) via a single-mode fiber optic cable to achieve a beam diameter of about 0.8 mm. A compact laser diode mount (LDM9LP, Thorlabs) was used to protect the pigtail from physical damage while also offering an excellent temperature regulation. The design of the mount reduces the thermal gradient across the laser diode, while its cold block cradles the pigtail housing for excellent heat transfer. Both the 405 nm and 635 nm laser diodes were driven in constant-current mode using two laser diode controllers (LDC501, Stanford Research Systems).

Both the detection and excitation laser beams were brought to the same optical path via a dichroic mirror (DMLP550T, Thorlabs) oriented 45° to the optical path of the microscope objective lens. A quarter-wave plate (WPMQ05M-633, Thorlabs) allowed the detection laser beam reflected at the back of the cantilever to be directed to the position-sensitive photodiode (PSPD) [28]. The proposed architecture simplifies the design of the otherwise complicated scan head in order to accommodate the extra optical components in addition to achieving the desired compactness.

In order to achieve the needed tight focusing of the laser beams, we used a microscope objective lens (LUCPlanFLN 20X, Olympus) with a working distance of about 7.5 mm. A beamsplitter partially split the reflected laser beam to a CCD camera for viewing the focused laser spot at the back of the cantilever during the laser alignment process. A four-quadrant photodiode (QP5-6 TO, First Sensor) with a low capacitance and small dark current was used to detect the vertical and horizontal deflections of the cantilever.

2.2. Mechanical design and Z-collar

The scan head is the major component of the PHS-AFM. Distinctly, the scan head has two main parts: the optics mount and the Z-collar. The proposed optics mount ensures that the detection (635 nm) and the excitation (405 nm) lasers are

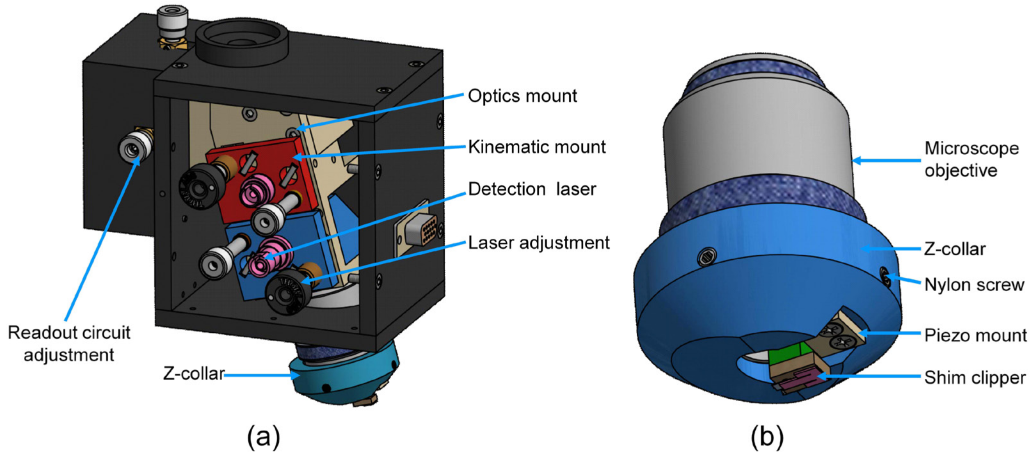

Figure 2. (a) 3D CAD model showing the various parts of the PHS-AFM scan head, (b) 3D CAD model of the Z-collar mounted on Olympus microscope objective lens (LUCPlanFLN 20X).

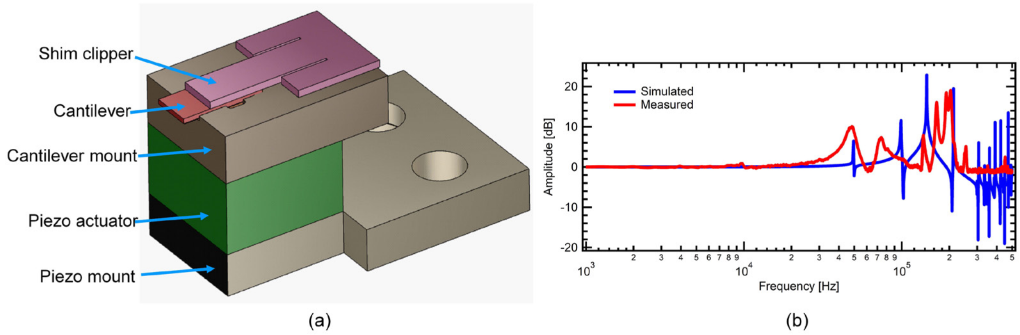

Figure 3. (a) The 3D CAD model of the Z-scanner with the cantilever mounted in place, (b) simulated and measured frequency response analyses of the Z-scanner with the first peak corresponding to mode I occurring at 49.51 kHz and 48.33 kHz, respectively.

brought to the same optical path for ease of alignment at the back of the cantilever and also allows the accurate detection of cantilever vibrations using the optical beam bounce detection (OBD) technique [29, 30]. On the other hand, the Z-collar contains the high-bandwidth Z-scanner with the cantilever mount. The mechanical parts used to mount various optics in the PHS-AFM scan head were primarily designed and fabricated from stainless steel owing to its low-temperature expansion coefficient. The kinematic mounts provide a simple means for centering the excitation laser at the base of the cantilever and the detection laser close to the free end of the cantilever. Figure 2(a) shows the assembled 3D CAD model.

One of the merits of our PHS-AFM lies in the simplistic design principle of our Z-scanner. Directly mounting the Z-collar onto the microscope objective lens allows the Z-scanner to be very minimal in design and prevents much unnecessary mass loading to the Z-scanner. It also enables the physical separation of the XY- and the Z-scanners. This has the benefit of maximizing the bandwidth of the Z-scanner and practically eliminating the cross-coupling of motions between the XY- and Z-axes. The assembled 3D model of the Z-collar mounted to the microscope objective lens, showing the various components, is shown in figure 2(b). A piezo mount is secured onto the Z-collar by using a couple of screws with a piezo chip firmly glued to it. The cantilever mount is then glued to the piezo chip. This overall design allows a cantilever

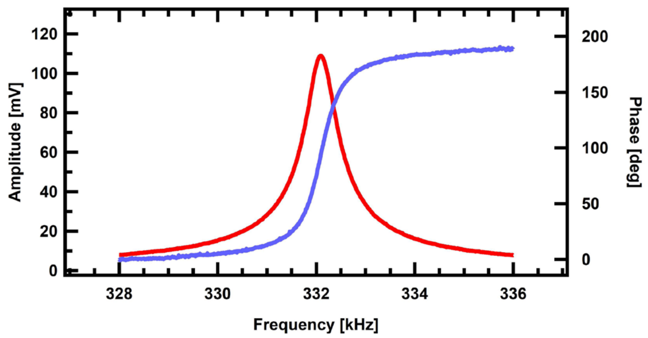

Figure 4. The first resonance curve (332 kHz) of a photo-thermally excited tapping mode cantilever (RTESPA7, Veeco. Inc).

to be firmly held. The cantilever is sandwiched between the recess on the cantilever mount and a shim clipper spot-welded to the mount. The illumination of the sample and the cantilever was achieved by a light-emitting diode (LED) mounted in a slot on the Z-collar.

2.3. Z-scanner

We adopted a simple design of attaching the Z-scanner onto the Z-collar, which is then directly mounted on a microscope objective lens. The Z-scanner is driven by piezoelectric chip (PA4FKW, Thorlabs) of size (5.0 mm × 5.0 mm × 3.0 mm).

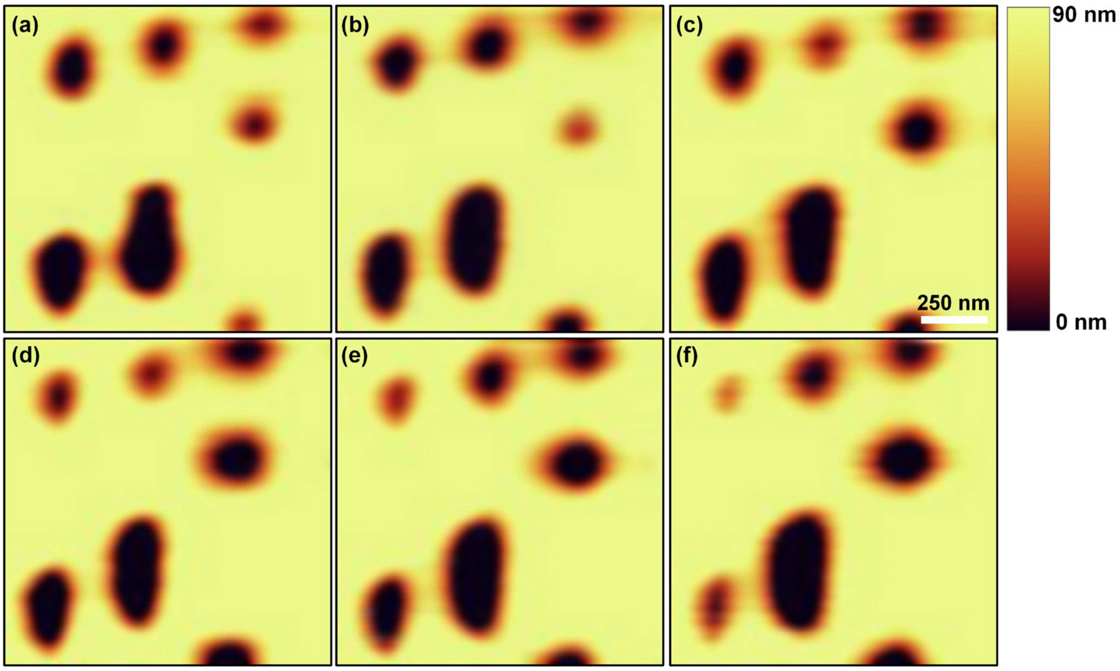

Figure 5. Images of Blu-ray data tracks obtained in air using our home-built PHS-AFM scan head in tapping mode. A scan size of 1 µm × 1 µm was used at a resolution of 128 pixels × 128 pixels for different imaging speeds. (a) 5 Hz, (b) 10 Hz, (c) 20 Hz, (d) 30 Hz, (e) 40 Hz and (f) 50 Hz. The scale bar is 250 nm.

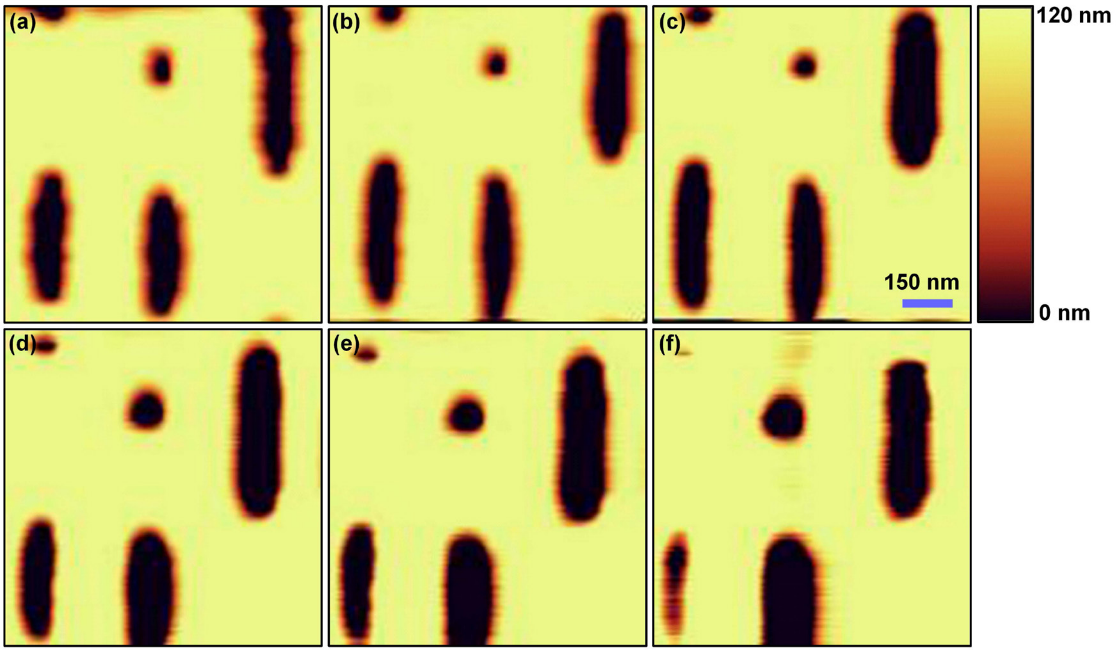

Figure 6. AM-AFM contact mode images of a Blu-ray disc obtained by using the developed PHS-AFM in air at different scan speeds (10, 20, 40, 60, 80, 100 lines/s respectively). The images were obtained using a NP-S cantilever from Bruker AFM Probes. Scan size of 0.8 µm × 0.8 µm. Pixel size: 128 × 128.

Figure 3(a) shows the 3D CAD model of the Z-scanner with the cantilever mounted in place.

In order to determine the characteristics of the Z-scanner we first used finite element analysis (FEA) to numerically determine the vibrational modes and associated frequencies. The Young's modulus, Poisson ratio, density, and the coupling coefficients of the piezo chip required for simulation were obtained from the manufacturer. The first four (4) vibration modes of the Z-scanner obtained by finite element analysis were 47.98 kHz, 48.61 kHz, 67.34 kHz and 96.96 kHz, respectively.

The AC response of the Z-scanner was also approximated using FEA, as shown in figure 3(b). From the simulated frequency response graph, there are multiple peaks that seem to be closely related to the vibrational modes of the Z-scanner. The first peak that corresponds to mode I (47.98 kHz) in the modal analysis was slightly higher and occurred at 49.51 kHz. The actual characteristics of the Z-scanner were measured using a home-built experimental set-up involving fiber optic interferometry. The piezo actuator was excited with a sine wave of amplitude 200 mV at frequencies between 1 and 500 kHz using our custom-written LabVIEW FPGA program. The first peak, corresponding to mode I in the modal analysis, was slightly lower than the simulated value (49.51 kHz) and occurred at 48.33 kHz. The maximum scan range measured using the same set-up was 2.2 µm.

2.4. Imaging

The scanning performance of the developed PHS-AFM was evaluated in tapping and contact modes using a commercial high-speed scanning probe microscope (SPM) controller. Imaging a Blu-ray disk having a pitch of about 320 nm was conducted in air with the XY- and Z-scanners operated in an open-loop control configuration.

Before imaging in tapping mode, one of the prerequisites is to measure the frequency response of the cantilever to obtain the operating frequency and amplitude. Therefore we obtained the cantilevers (RTESPA7, Veeco. Inc) response by photo-thermally exciting the 405 nm laser and the cantilever vibration response measured by using the optical beam bounce technique. Both the amplitude and phase versus the frequency curves of the flexural mode of the cantilever are shown in figure 4. The results show that the blue laser is capable of exciting the tapping mode cantilever without stirring unnecessary resonances, and therefore it can be used effectively for frequency modulation AFM.

We then performed high-resolution imaging by using the tapping mode cantilevers (RTESPA7, Veeco. Inc) with a spring constant of between 20–80 N m^{-1}. A scan size of 1 µm × 1 µm was used at a resolution of 128 × 128 pixels. Figure 5 shows the raw topographic images of a Blu-ray disk obtained with the developed PHS-AFM in amplitude modulation (AM) mode. With the current set-up, we are able to obtain images at about 50 Hz before the appearance of a significant degradation in the quality of the images. Nonetheless, the unfilled track pits are still clearly distinguishable at 50 Hz, confirming that the developed scan head is capable of high-speed imaging.

Similarly, contact mode imaging was performed with triangular cantilevers (NP-S, Bruker). The scan size of 0.8 µm × 0.8 µm at the resolution of 128 × 128 pixels was used. The sequence of consecutive images of the topography acquired at different scanning speeds are shown in figure 6. From the images, there is no discernible deterioration even at 100 Hz (about 1 frame per second). The track pits on the Blu-ray disk surface can be accurately followed by our Z-scanner.

3. Conclusions

We have presented a comprehensive description of the design and development of a PHS-AFM scan head with a means of photo-thermally exciting a cantilever. The elegant design of our Z-scanner provides a relatively large stroke (2.2 µm) with a large bandwidth suitable for many high-speed imaging applications. The efficacy of our developed scan head was evaluated by imaging a piece of a Blu-ray disk in both contact and tapping modes. We have been able to perform high-speed AFM imaging up to 100 Hz in contact mode. Also, the effectiveness of remotely exciting the cantilever by using the photo-thermal effect was demonstrated by imaging in tapping mode. We believe that imaging speed in our current set-up is limited by the bandwidth of the commercial controller in the loop. We are in the process of developing our own high-speed controller to improve the scanning speed in the future.

Acknowledgment

This research was supported by the Basic Science Research Program through the National Research Foundation of Korea (NRF) funded by the Ministry of Science and ICT (Grant No. NRF-2018R1A2B6008264).

ORCID iDs

Bernard Ouma Alunda https://orcid.org/0000-0003-0283-6525
Luke Oduor Otieno https://orcid.org/0000-0003-3129-2010
Sang Joon Park https://orcid.org/0000-0002-3259-1074
Si Geun Choi https://orcid.org/0000-0001-8209-8571
Jong Hyoung Kim https://orcid.org/0000-0002-7217-4347
Yong Joong Lee https://orcid.org/0000-0001-5254-8041

References

[1] Herruzo E T, Perrino A P and Garcia R 2014 Fast nanomechanical spectroscopy of soft matter *Nat. Commun.* **5** 3126
[2] Gao Y, Wang J, Zhong J, Wang Y, Yin Q, Hou B and Hao H 2017 Application of atomic force microscopy in understanding crystallization process *Sci. Adv. Mater.* **9** 89–101
[3] Iyer S, Gaikwad R M, Subba-Rao V, Woodworth C D and Sokolov I 2009 AFM detects differences in the surface brush of normal and cancerous cervical cells *Nat. Nanotechnol.* **4** 389–93
[4] Lekka M 2012 Atomic force microscopy: a tip for diagnosing cancer *Nat. Nanotechnol.* **7** 691–92
[5] Revenko I, Tang Y and Santerre J 2001 Surface structure of polycarbonate urethanes visualized by atomic force microscopy *Surf. Sci.* **491** 346–54
[6] Deng Z, Lulevich V, Liu F T and Liu G Y 2010 Applications of atomic force microscopy in biophysical chemistry of cells *J. Phys. Chem.* B **114** 5971–82
[7] Kozhukhov A S, Sheglov D V and Latyshev A V 2017 Reversible electrochemical modification of the surface of a semiconductor by an atomic-force microscope probe *Semiconductors* **51** 420–22
[8] Oyabu N, Sugimoto Y, Abe M, Custance Ó and Morita S 2005 Lateral manipulation of single atoms at semiconductor surfaces using atomic force microscopy *Nanotechnology* **16** S112–7

[9] Kodera N, Yamamoto D, Ishikawa R and Ando T 2010 Video imaging of walking myosin V by high-speed atomic force microscopy *Nature* **468** 72–6
[10] Ando T, Kodera N, Naito Y, Kinoshita T, Furuta K and Toyoshima Y 2003 A high-speed atomic force microscope for studying biological macromolecules in action *ChemPhysChem* **4** 1196–202
[11] Huang Q, Wu H, Cai P, Fein J B and Chen W 2015 Atomic force microscopy measurements of bacterial adhesion and biofilm formation onto clay-sized particles *Sci. Rep.* **5** 16857
[12] Gorham N, Becker T, Shiers D W and Watling H R 2009 Visualisation of bacterial behaviour using tapping-mode atomic force microscopy *Adv. Mat. Res.* **71** 341–4
[13] Kim K S, Cho C H, Park E K, Jung M H, Yoon K S and Park H K 2012 AFM-detected apoptotic changes in morphology and biophysical property caused by paclitaxel in Ishikawa and HeLa cells *PLoS One* **7** e30066
[14] Lekka M 2016 Discrimination between normal and cancerous cells using AFM *Bionanoscience* **6** 65–80
[15] Braunsmann C, Seifert J, Rheinlaender J and Schaffer T E 2014 High-speed force mapping on living cells with a small cantilever atomic force microscope *Rev. Sci. Instrum.* **85** 073703
[16] Kitazawa M, Shiotani K and Toda A 2003 Batch fabrication of sharpened silicon nitride tips *Japan. J. Appl. Phys.* **42** 4844–7
[17] Fantner G E, Schitter G, Kindt J H, Ivanov T, Ivanova K, Patel R and Hansma P K 2006 Components for high speed atomic force microscopy *Ultramicroscopy* **106** 881–7
[18] Ando T, Uchihashi T and Fukuma T 2008 High-speed atomic force microscopy for nano-visualization of dynamic biomolecular processes *Prog. Surf. Sci.* **83** 337–437
[19] Hansma P K, Schitter G, Fantner G E and Prater C 2006 High-speed atomic force microscopy *Science* **314** 601–2
[20] Viani M B, Schääffer T E, Chand A, Rief M, Gaub H E and Hansma P K 1999 Small cantilever for force spectroscopy of single molecules *J. Appl. Phys.* **86** 2258–62
[21] Revenko I and Proksch R 2000 Magnetic and acoustic tapping mode microscopy of liquid phase phospholipid bilayers and DNA molecules *J. Appl. Phys.* **87** 526–33
[22] Florin E L, Radmacher M, Fleck B and Gaub H E 1994 Atomic force microscope with magnetic force modulation *Rev. Sci. Instrum.* **65** 639–43
[23] Xu X and Raman A 2007 Comparative dynamics of magnetically, acoustically, and Brownian motion driven microcantilevers in liquids *J. Appl. Phys.* **102** 034303
[24] Carbone G, Pierro E and Soria L 2009 Microcantilever dynamics: Effect of Brownian excitation in liquids *Proc. SEM Annual Conf. and Exposition on Experimental and Applied Mechanics* pp 63–9
[25] Umeda K, Oyabu N, Kobayashi K, Hirata Y, Matsushige K and Yamada H 2010 High-resolution frequency-modulation atomic force microscopy in liquids using electrostatic excitation method *Appl. Phys. Express* **3** 065205
[26] Kiracofe D and Raman A 2011 Quantitative force and dissipation measurements in liquids using piezo-excited atomic force microscopy: a unifying theory *Nanotechnology* **22** 485502
[27] Nishida S, Kobayashi D, Kawakatsu H and Nishimori Y 2009 Photothermal excitation of a single-crystalline silicon cantilever for higher vibration modes in liquid *J. Vac. Sci. Technol.* **27** 964–8
[28] Schaffer T E, Cleveland J P, Ohnesorge F, Walters D A and Hansma P K 1996 Studies of vibrating atomic force microscope cantilevers in liquid *J. Appl. Phys.* **80** 3622–7
[29] Meyer G and Amer N M 1988 Novel optical approach to atomic force microscopy *Appl. Phys. Lett.* **53** 1045–7
[30] Hosaka S, Etoh K, Kikukawa A and Koyanagi H 2000 Megahertz silicon atomic force microscopy (AFM) cantilever and high-speed readout in AFM-based recording *J. Vac. Sci. Technol.* B **18** 94–9